Fachtagung "Experimentelle Strömungsmechanik"
6-8. September 2022, Ilmenau

Bildung von Strömungsstrukturen in einem gegenrotierenden Taylor-Couette System mit sehr weitem Spalt (η = 0.1)

Formation of flow patterns in a counter-rotating very wide gap Taylor-Couette flow (η = 0.1)

Mohammed Hussein Hamede[1], Sebastian Merbold[1], Christoph Egbers[1]
[1]Lehrstuhl Aerodynamik und Strömungslehre, Brandenburgisch Technische Universität Cottbus-Senftenberg, Siemens-Halske-Ring 15a, 03046 Cottbus, Deutschland

Keywords: Very wide gap Taylor-Couette, turbulence, PIV, Taylor vortices

Abstract

In this study, we investigate the turbulent Taylor-Couette flow experimentally. First, in order to show the formation of the different patterns in the flow, the flow was seeded with kalliroscope particles and by applying a vertical laser sheet we were able to capture the different patterns in the flow. For a further detailed study, the flow field was measured in horizontal planes at different cylinder heights using Particle image velocimetry (PIV). The formation of patterns appears for the counter-rotation configuration where the outer cylinder rotates in the opposing direction of the inner cylinder rotation. For low shear Reynolds numbers, stable Taylor vortices fulfilling the whole gap appear for very low counter-rotation rates. While for the same rotation rates and higher shear Reynolds number new patterns appear, which we can describe as interlaced fingers from in and outflow, where in the angular momentum transport a maximum occurs due to a formation of these patterns.

Introduction

The flow in the gap between two independently rotating coaxial cylinders is widely studied for more than one century. The geometry of the TC system is defined by its radius ratio $\eta=r_1/r_2$ and the aspect ratio $\Gamma=L/d$ with the cylinder length L, the cylinder radii r_1 and r_2 for the inner and outer ones, and the gap width $d=r_2-r_1$. The system is driven by angular velocities ω_2 and ω_1 of the outer and inner cylinders respectively, resulting in the ratio of angular velocities $\mu=\omega_2/\omega_1$ and the shear Reynolds number $Re_S=2r_1r_2(r_2-r_1)|\omega_2-\omega_1|/(\nu(r_1+r_2))$ (Dubrulle et al. 2005), where ν represents the kinematic viscosity.
The simple Taylor Couette geometry, and the ability to control the flow by changing the different parameters, attract the scientist to study different topics like flow instabilities, formation of patterns, angular momentum transport, etc… The Visualization of the flow produces fascinating patterns which vary in different ways by changing the rotation rate of the cylinders and also by changing the aspect ratio of the apparatus. The changing of the driving parameters leads to a series of flow transitions, these flow transitions can be classified into different flows, like circular Couette flow, Taylor vortex flow, periodic nonaxisymmetric flow, wavy vortex flow, modulated wavy vortex flow, etc.. (Taylor (1923); Andereck (1986); Lim et al. (1998)).

GALA e.V., Karlsruhe, Germany, ISBN 978-3-9816764-8-8

The transport of angular momentum in TC flows can be quantified by the quasi Nusselt number Nuω which can be measured by measuring the torque T acting on the cylinder walls according to Eckhardt et al (2007b). For fixed Re_S flow the torque exhibits a maximum for low counter-rotating regimes, and this was investigated for the flow in different geometries with different aspect rations [Van Gils et al. (2012) for η=0.71, Merbold et al. (2013), Froitzheim et al.(2017) for η=0.5, Froitzheim et al.(2019b) for η=0.357]. In the flow field, this maximum is accompanied by a flattening of the angular velocity profile and strengthening or rather forming of large scale vortices [Van Gils et al. (2012),Ostilla-Mónico et al. (2013, 2014a,b), Merbold et al. 2014 , Van der Veen et al. (2016), Froitzheim et al.(2017), Froitzheim et al.(2019a)].
In this study, we will present the results from the visualization done for the Taylor-Couette flow with a radius ratio of 0.1 where different patterns appeared. Also, we perform PIV measurements in the radial-azimuthal plane at different axial positions to quantify the velocity field and therefore show the existence of the different patterns, and how the existence of these patterns affects the angular momentum transport which was calculated from the measured velocity field.

Experimental Setup and Measurement procedure

In the current study, we used the Top view Taylor Couatte (TvTC) - Cottbus facility, this facility has a changeable inner cylinder, so with that, we can study different TC geometries using this apparatus (van der Veen et al. (2016), Froitzheim et al. (2017), Froitzheim et al. (2019)).
I our investigation, we used the inner cylinder of r_1= 7mm and with the fixed outer cylinder with r_2 = 70mm, leading to a radius ratio of η = 0.1 and a gap width of d = r2 − r1 = 63 ± 0.2mm. The apparatus is 70 cm long, leading to aspect ratio Γ = L / d = 11.11. Every cylinder is connected to a DC motor via a gear transmission belt, so both cylinders can rotate independently.

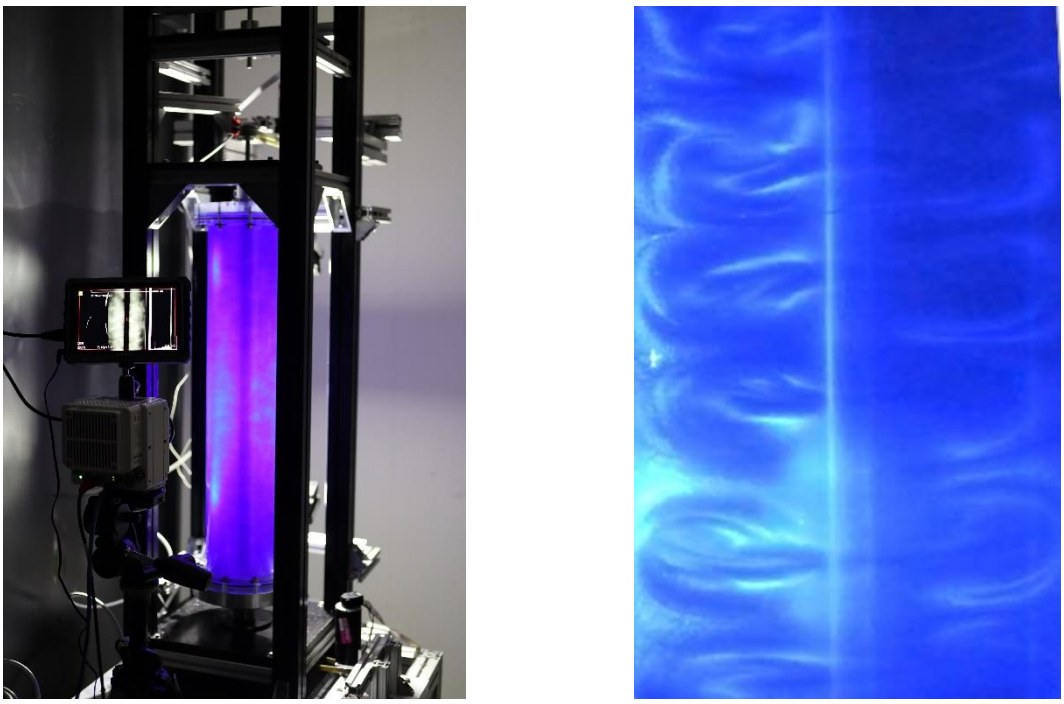

Fig. 1: Sketch of the Taylor-Couette geometry with the visualization set up (left) and image of the visualized stable Taylor vortices for Re_S = 850 and μ=-0.01.

GALA e.V., Karlsruhe, Germany, ISBN 978-3-9816764-8-8

The transparent outer cylinder (OC) and the top plate are made of acrylic glass to enable optical access to the flow. Both end plates are fixed to the outer cylinder and rotate at the same speed.
For the visualization, we used silicone oil as a working fluid. Different kinds of silicone oil with different viscosity were used (ϑ(@ 25 °C)=0.65, 5.4, 10.34 mm^2/s). The fluid was seeded with kalliroscope particles and subjected to a vertical laser sheet, and a camera was placed on the side which allows us to capture the radial-axial flow as shown in figure 1. So that by Capturing the particle light reflections we can analyze the flow patterns occurring in the system.
Figure 2 shows the PIV setup used in this study. A Pahntom veo 640l (2560x1600 pixels) high-speed camera was mounted on the top of the apparatus, and a LDY.300PIV laser (λ = 532nm, P = 15mJ) was placed beside the apparatus, and the laser output was transported using a guiding arm, by this it can generate a horizontal laser sheet through the gap as shown. The position of the laser sheet was adjustable, which allow us to measure the flow velocities at different heights (analogy to Froitzheim et al.(2017), Froitzheim et al.(2019a)). The measurement itself consists of 2000 images recorded at 200 Hz at each axial position, allowing time-resolved velocimetry. Experiments and post-processing were done with the software Davis from LaVision with a final interrogation area size of 24 x 24 pixels and 50% overlap was used to reach a spatial resolution of (0.653 µm\pixel – 0.8129 µm\pixel).

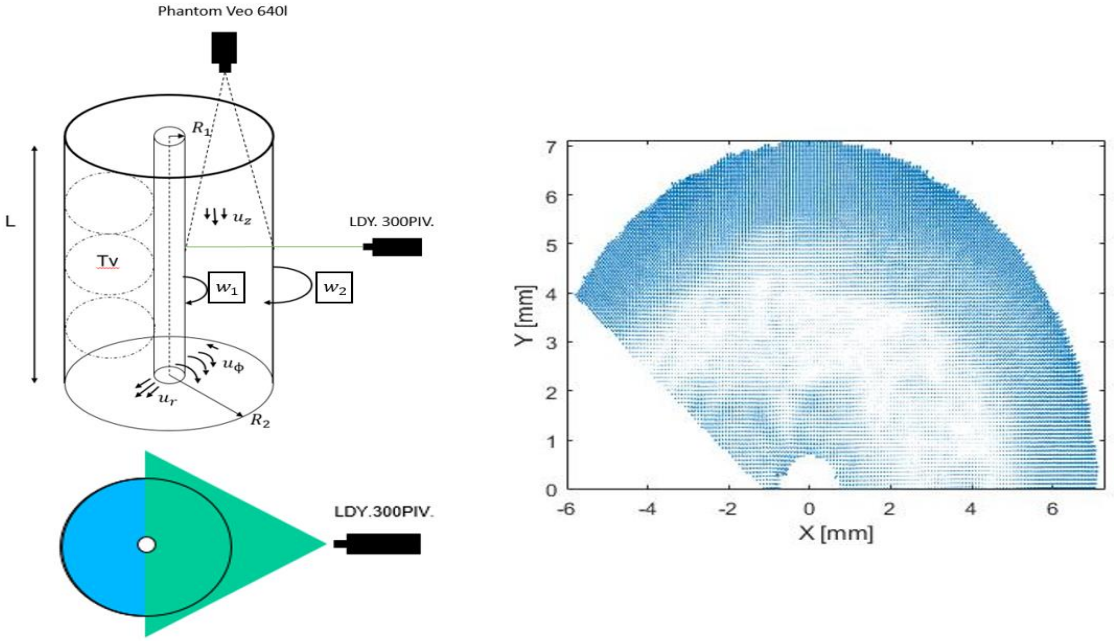

Fig. 2: To the left: Schematic sketch showing the vertical cross-section of the TC apparatus with the PIV setup, and the horizontal cross-section of the setup with the horizontal laser sheet. To the right: Instantaneous Velocity field in the azimuthal-radial plane at mid-height obtained using PIV.

Flow visualization

For the visualization, we used the same TC setup explained in the previous section, but two different cameras, so for the low Reynolds number, where we observe stable flow patterns, we capture the flow with Canon EOS 1100D camera with a frame rate of 25 fps. While for the high shear Reynold number the patterns are getting more time-dependent, we used the Phantom veo 640 fast speed camera with a frame rate 300 fps. Figure 3 shows the existence of stable

GALA e.V., Karlsruhe, Germany, ISBN 978-3-9816764-8-8

Taylor vortices (TV) for low Re_S = 530 at a very low counter-rotation rate μ=-0.01. Then by increasing the counter-rotation rate it's clear how this TV detaches from the outer cylinder and is more concentrated in the region next to the inner cylinder. These results are in agreement with different previous studies (Van der Veen et al. (2016), Froitzheim (2017)), where they showed that for high counter-rotating rates the outer cylinder stabilizes the flow in the outer region, so the flow patterns detach from it. But in the current study, we observe that for this very wide geometry by increasing the counter-rotation rates the axial wavelength of the patterns decreases as shown in figure 3, it is clear that the number of vortices counted for μ=-0.01 increases once we increase the counter-rotation rate.

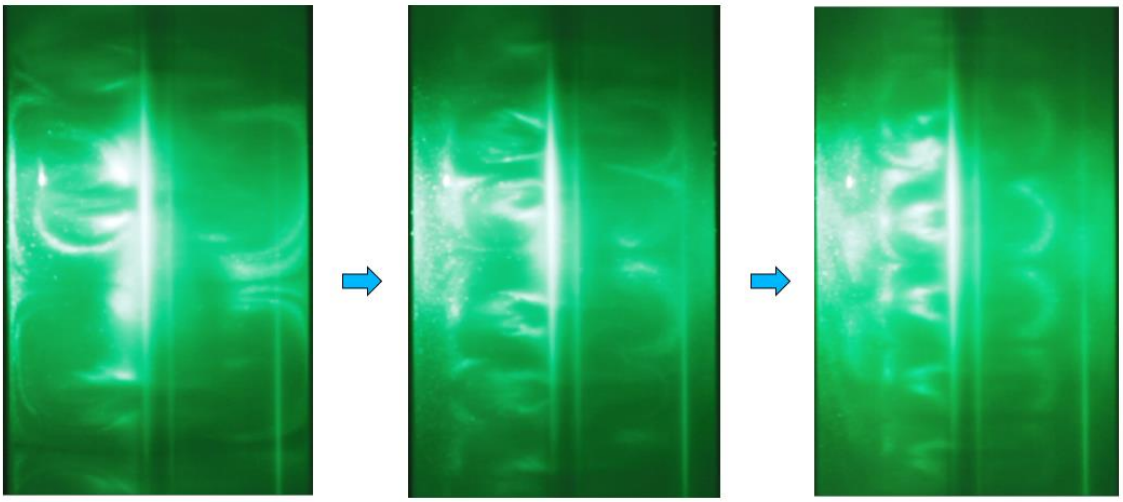

Fig 3: From the left to the right: The detachment of the flow patterns from the outer cylinder by increasing the counter-rotating rate for Re_S= 530.

Calibration

For the calibration related to the PIV measurements, using a calibration target in order to do a regular calibration procedure is not possible, as the calibration target has to be placed inside the apparatus. In order to remove it from the apparatus, we would need to disassemble the top plate and the camera placed above the top plate, which leads to losing the calibration after resembling the apparatus again. It is not possible to replace them accurately in their previous positions due to the complexity of the facility.
For this reason, we detect the location of the inner and outer cylinder in image coordinates and by fitting the system's coordinates to the illuminated walls in the images. Using the position of the center of both cylinders we can calibrate our measurements. Figure 4 (left) shows to the left an instantaneous PIV image, from this image we can detect the light reflection from both the inner and the outer cylinder walls. As the borders of the inner and outer cylinder are clear, we fit two concentric circles through the IC and OC walls.
Figure 4 (right) shows in red the fitted concentric circles to the OC and IC, where the ratio of the radius of the fitted circle around the inner cylinder to the radius of the fitted circle around the outer cylinder is 0.1 which is equal to the real radius ratio of the facility (η = 0.1).

GALA e.V., Karlsruhe, Germany, ISBN 978-3-9816764-8-8

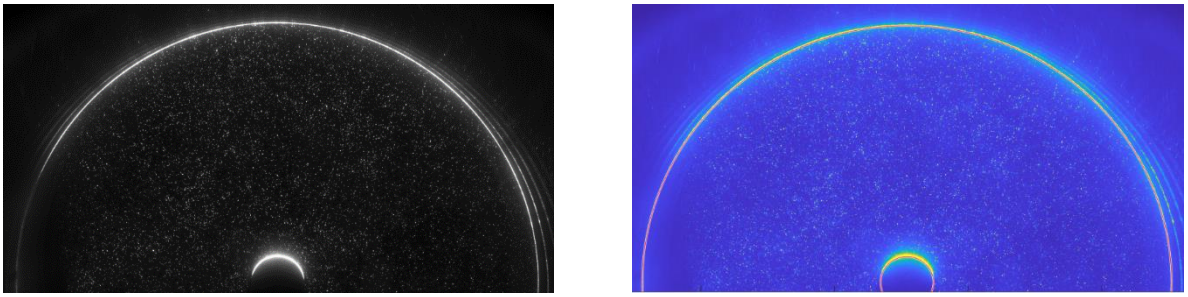

Fig. 4: To the left: PIV image at one instantaneous time, To the right: The red lines represent the best fit of concentric circles through the cylinder points. Height of horizontal plane: z-L/2=40 mm.

Here we should mention that the PIV algorithm performed on the images is in image coordinates (unit in pixel), resulting velocities are computed also in image coordinates (units in px-displacement). In order to transform our output velocities to real coordinates (units in m and m/s), and after finding the image coordinates of the fitted concentric circles' center we calculate our spatial resolution (mm/pixel), by determining the known gap width (63mm) in image coordinates (unit in pixel). This procedure was done for the 21 different measured heights, so by adjusting the laser sheet height, the camera lens was refocused to capture the flow at the desired height with higher possible resolution and clarity, and new spatial resolution is measured. Furthermore, the velocity data is transformed using MATLAB 2019b to a polar coordinate velocity (U_r, U_ϕ) and interpolated onto a polar grid of concentric cylinders of fixed radii r, where the azimuthal φr displacement is taken constant for all r using the displacement of vectors of the original cartesian grid.
The time resolved planar PIV in φr planes at different 21 heights. Leads to understanding statistically the three dimensional flow.

Axial-dependent velocity field

In order to study the influence of the rotation ratio on the flow inside the Taylor Couette (TC) apparatus, and to investigate the results shown in Figure 3 for flows with higher shear Reynolds numbers, the radial and azimuthal velocity components were measured using PIV technique. As its mentioned above the measurements were done at different axial positions. The contour plot shows the variation of the mean radial and azimuthal velocities across time and the azimuthal coordinate direction for Re_s=2·10^4 and rotation ratios μ=-0.06 and at 21 different measured heights with 5 mm differences between each height, with 3 heights above the apparatus midheight and 18 below.
We observe an obvious variation of the radial velocity along the different heights, where in- and outflow regions exist. In agreement with the results shown in figure 3, these radial velocities are concentrated in the area next to the inner cylinder, while the effect of the outer cylinder rotation in the opposite direction of the inner one appears to stabilize the flow. The consequence is the disappearance of the radial velocity in the region next to the outer cylinder. These in and out flow regions can be a fingerprint of a rotating pattern in the gap, like those observed by Froitzheim et al. (2017).

GALA e.V., Karlsruhe, Germany, ISBN 978-3-9816764-8-8

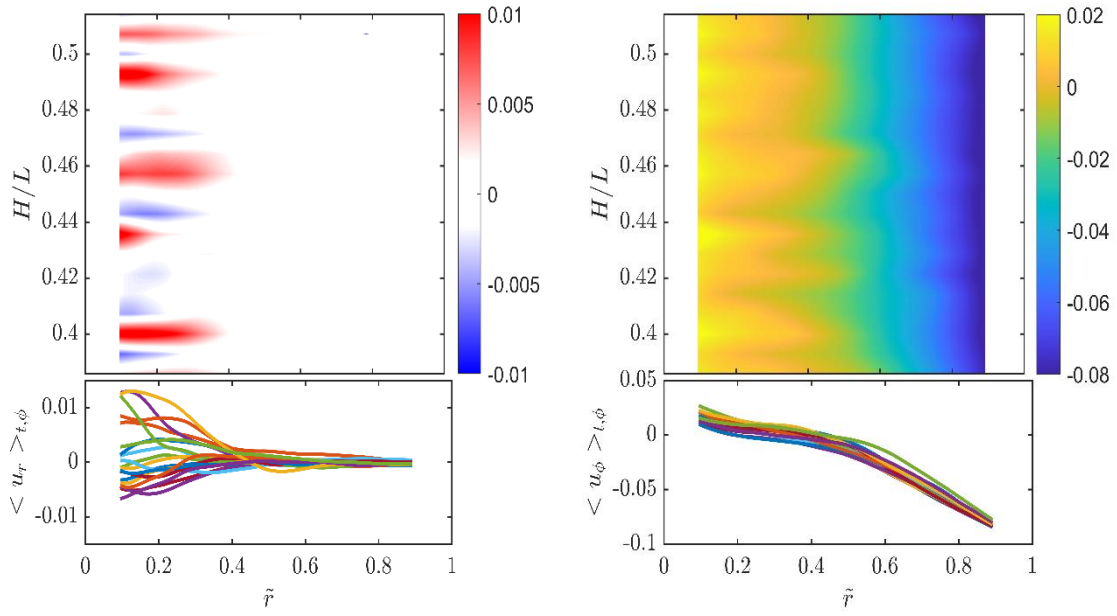

Fig. 5: left: Contour plots and velocity profiles of the azimuthally and time-averaged radial velocity components, right: Contour plots and velocity profiles of the azimuthally and time-averaged azimuthal velocity components, for $Re_S=2\cdot10^4$ and rotation ratios μ=-0.06. Each contour plot consists of 21 height measurements separated by 5 mm in the axial coordinate direction. The color map unit is (m/sec).

In contrast, in the here observed case the thickness of these regions is axially short, so they can't be described as a classical Taylor vortices, but we can understand them as interlaced fingers from in and outflow, where these patterns fulfill the whole gap. Where this pattern fulfills the whole gap for low counter rotations rates (μ=-0.011) as it is the case with the Taylor vortices shown in figure 3, and then started to detach from the outer wall for higher counter-rotation rates.

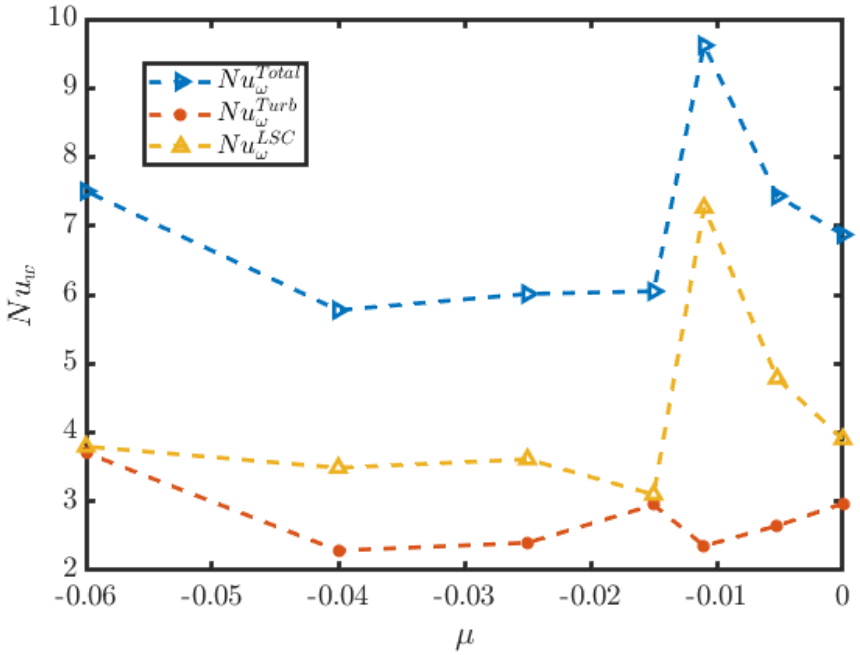

Fig. 6: The variation of the Radial averaged Nusselt number turbulent and large scale contributions for Re_s =20000 and different rotation ratios.

GALA e.V., Karlsruhe, Germany, ISBN 978-3-9816764-8-8

The azimuthal velocity also shows how the axial dependence of the azimuthal velocity profiles is restricted to the inner region of the gap, where the rotating patterns exist. While in the outer region we can observe how the flow is stabilized by the rotation of the outer cylinder, where we can just observe a radial dependence and the velocity profile tends to be linear.
The radial velocity component shows clearly large-scale vortices with an inflow region transporting fluid from the outer to the inner cylinder and an outflow region with the reverse orientation. We defined the radial velocity component to be positive in the outflow region. In order to study how the existence of patterns affects the angular momentum transport. The variation of the Nusselt number with respect to the different rotation ratios is shown in figure 6. It is clear from the figure that Nu_ω achieve a maximum for the low counter rotating regimes.

For a more detailed study, the flow was decomposed into Large scale and turbulent contributions according to Brauckmann & Eckhardt (2013)

$$u = < u >_{\phi,t} + u' = \bar{u} + u'$$

Using this decomposition, we were able to calculate the Large scale Nu_ω^{LSC} and the turbulent contributions Nu_ω^{Turb} to the Nusselt number:

$$Nu_\omega^{Turb} = J_{lam}^{-1} < r^3 < u_r' \omega' >_{A(r),t} >_r$$
$$Nu_\omega^{LSC} = J_{lam}^{-1} < r^3 (< \bar{u}_r \bar{\omega} >_{A(r),t} - \vartheta \partial_r < \bar{\omega} >_{A(r),t}) >_r$$

It is shown clearly in figure 5 that for very low counter-rotating ratios where the patterns exist and fulfill the hole gap as shown in the contour figures the large-scale contribution of the Nusselt number is the maximum. And for the same rotation ratio where the total Nusselt number achieves the maximum, the large-scale circulation contribution is the maximum which shows a clear relationship between the existence of these patterns and the increase in the angular momentum transport. So these patterns enhance the angular momentum transport in agreement to the findings related to Taylor Couette flows with different geometries (Merbold et al. (2013), Froitzheim et al.(2017) for η=0.5, Froitzheim et al.(2019) for η=0.357).

Acknowledgments

We gratefully acknowledge financial by Deutsche Forschungsgemeinschaft (e DFG EG100/23-1 and EG100/30- 1).

Literature

Andereck C.D., Liu S.S., Swinney H.L., 1986: “Flow regimes in a circular Couette system with independently rotating cylinders”, J. Fluid Mech. 164:155–83

Brauckmann, H.J. and Eckhardt, B., 2013a: “Direct numerical simulations of local and global torque in Taylor Couette flow up to Re=30000”, J. Fluid Mech., 718:398-427

GALA e.V., Karlsruhe, Germany, ISBN 978-3-9816764-8-8

Brauckmann, H. J. and Eckhardt, B., 2013b: “Intermittent boundary layers and torque maxima in Taylor-Couette flow”, Phys. Rev. E 87, 033004

Dubrulle, B., Dauchot, O., Daviaud, F., Longaretti, P.-Y., Richard, D. and Zahn, J.-P., 2005: “Stability and turbulent transport in Taylor–Couette flow from analysis of experimental data”, Phys. Fluids 17, 095103

Eckhardt, B., Grossmann, S. and Lohse, D., 2007a: “Fluxes and energy dissipation in thermal convection and shear flows”, Europhys. Lett. 78, 24001

Eckhardt, B., Grossmann, S., Lohse, D.,2007b: “Torque scaling in turbulent Taylor-Couette flow between independently rotating cylinders”, J. Fluid Mech. 581, 221

Froitzheim, A., Merbold, S. & Egbers, C. 2017 Velocity profiles, flow structures and scalings in a wide-gap turbulent taylor-couette flow. J. Fluid Mech. 831, 330–357.

Froitzheim, A., Ezeta, R., Huisman, S. G. & Merbold, S., Sun C. Lohse D. Egbers C. 2019a Statistics, plumes and azimuthally travelling waves in ultimate taylor-couette turbulent vortices. J. Fluid Mech. 876, 733–765.

Froitzheim, A., Merbold, S., Ostilla-Monico, R. & Egbers, C. 2019b Angular momentum transport and flow organization in taylor-couette flow at radius ratio of η = 0.357. Phys. Rev. 084605, 53:427.

Merbold, S., Brauckmann, H.J., Egbers, Ch.,2013: “Torque measurements and numerical determination in differentially rotating wide gap Taylor-Couette flow”, Phys. Rev. E 87, 023014

Merbold, S., Froitzheim, A., Egbers, C., 2014: “Flow pattern and angular motion transport in a wide gap Taylor-Couette flow”, TU Dresden, Strömungstechnische Tagung 2014, Schriftenreihe aus dem Institut für Strömungsmechanik Band 10

Lim, T. T., Chew, Y. T. & Xiao, Q. 1998 A new flow regime in a taylor-couette flow. phys. Fluids 10, 3233.

Taylor, G. I. 1923 Stability of a viscous liquid contained between two rotating cylinders. Phil. Trans. R. Soc. Lond. A 223, 289.

Ostilla, R., Stevens, R.J.A.M., Grossmann, S., Verzicco, R. and Lohse, D.,2013: “Optimal Taylor-Couette flow: direct numerical simulations”, J. Fluid Mech., 719: 14-46

Ostilla-Mónico, R., Huisman, S.G., Janninik, T.J.G., van Gils, D.P.M., Verzicco, R. et al.,2014a: “Optimal Taylor-Couette flow: radius ratio dependence”, J. Fluid Mech. 747:1-29

Ostilla-Mónico, R., van der Poel, E.P., Verzicco, R., Grossmann, S., Lohse, D.,2014b: “Exploring the phase diagram of fully turbulent Taylor-Couette flow”, J. Fluid Mech. 761:1–26

Van der Veen, R.C.A., Huisman, S.G., Merbold, S., Harlander, U., Egbers, Ch., Sun, C. and Lohse, D.,2016: “Taylor-Couette turbulence at radius ratio η=0.5: scaling, flow structures and plumes”, J. Fluid Mech., 799: 334-351

Van Gils, D. P. M., Huisman, S., Grossmann, S., Sun, C. and Lohse, D.,2012: “Optimal Taylor-Couette turbulence”, J. Fluid Mech. 706, 118.

GALA e.V., Karlsruhe, Germany, ISBN 978-3-9816764-8-8